



EDGES signal in presence of magnetic-fields

Pravin Kumar Natwariya ^{1,2*} and Jitesh R. Bhatt ^{1†}

¹Physical Research Laboratory, Theoretical Physics Division, Ahmedabad 380 009, India

²Indian Institute of Technology, Gandhinagar, Ahmedabad 382 424, India

18 June 2020

ABSTRACT

We study the 21-cm differential brightness temperature in the presence of primordial helical magnetic fields for redshift $z = 10 - 30$. We argue that the α -effect that sets in at *earlier time* can be helpful in lowering the gas temperature to 3.2 degrees Kelvin at $z = 17$. This effect can arise in the early Universe due to some parity violating high energy processes. Using the EDGES (Experiment to Detect the Global Epoch of Reionization Signature) results, we find the upper and lower limits on the primordial magnetic field to be 6×10^{-3} nG & 5×10^{-4} nG respectively. We also discuss the effect of Ly α background on the bounds. Our results do not require any new physics in terms of dark matter.

Key words: EDGES observation, Magnetic fields, 21-cm signal, Magnetohydrodynamics, first stars, dark matter

1 INTRODUCTION

Recently, the observations from the Experiment to Detect the Global Epoch of Reionization Signature (EDGES) has created enormous interest in 21-cm cosmology with a hope to provide an insight into the period when the first stars and galaxies were formed (Bowman et al. (2018); Pritchard & Loeb (2012)). The EDGES collaboration has reported nearly two times more absorption for the 21-cm line than the prediction made by the standard cosmological scenario based on the Λ CDM framework in the redshift range $15 \lesssim z \lesssim 20$ (Bowman et al. (2018)). Analysis of the results shows that the absorption profile is in a symmetric “U” shaped form centered at 78 ± 1 MHz. Minimum of the absorption profile reported being at $-0.5^{+0.2}_{-0.5}$ K in the above-mentioned redshift range. Inability of the standard scenario to explain the observations indicates a possibility of new physics. Any possible explanation may require that either the gas temperature, T_{gas} , should be less than 3.2 K for the standard cosmic microwave background radiation temperature (T_{CMB}) or T_{CMB} should be greater than 104 K in the absence of any non-standard mechanism for the evolution of the T_{gas} at the centre of the “U” profile for the best fitting amplitude (Bowman et al. (2018)).

First, it ought to be noted that in the standard cosmological scenario, during the cosmic dawn, T_{gas} and T_{CMB} varies adiabatically with the redshift as $T_{\text{gas}} \propto (1+z)^2$ and $T_{\text{CMB}} \propto (1+z)$. At redshift $z = 17$, temperatures of both the components found to be $T_{\text{gas}} \sim 6.8$ K & $T_{\text{CMB}} \sim 48.6$ K, for example see Ref. (Seager et al. (1999)). As explained above, one of the alternatives to explain the EDGES signal is by cooling the gas. In Refs. (Tashiro et al. (2014); Barkana (2018)), a Coulomb-like interaction

between the dark-matter and baryon was considered for transferring energy from gas to dark matter. This approach as argued in Ref. (Muñoz & Loeb (2018)), can violate constraints on local dark-matter density. At the required redshift ionization fraction is the order of, $x_e = n_e/n_H \sim 10^{-4}$. Therefore, the dominating part is neutral hydrogen and it possesses only dipole interactions instead of Coulomb-like interaction (Fraser et al. (2018); Bransden et al. (1958)). In addition, the non-standard Coulombic interaction between dark matter and baryons is strongly constrained by observations and laboratory experiments. In the light of these constraints, it is doubtful that one can produce 21-cm absorption signal using the Coulombic interaction (Barkana et al. (2018); Berlin et al. (2018); Kovetz et al. (2018); Muñoz et al. (2018); Slatyer & Wu (2018)). A new approach was recently adopted in Refs. (Mirocha & Furlanetto (2019); Ghara & Mellema (2019)) for the excess cooling of gas by introducing a new parametric model. This model allows the cooling to occur more rapidly at earlier times. However, the origin of the new cooling term remains uncertain. The excessive cooling of the gas can also be obtained by allowing thermal contact between baryons and cold dark matter-axions (Sikivie (2019)).

Another alternative to explain EDGES results requires extra radiation at the time of cosmic dawn. This possibility has been investigated by several authors. In Ref. (Fraser et al. (2018)), the authors consider extra radiation field in the required frequency range by light dark-matter decay into soft photons. In presence of the intergalactic magnetic fields, axion-like particles can be converted into photons under some resonant condition to generate the extra radiation (Moroi et al. (2018)). Similarly, resonant conversion of mirror neutrinos into visible photons can explain the EDGES observations (Aristizabal Sierra & Fong (2018)). In Ref. (Ewall-Wice et al. (2018)), it was suggested that black-holes growing at certain rates can also produce a radio background at the required redshift. However, this type of scenario of the first-stars and black-holes

* E-mail: pravin@prl.res.in

† E-mail: jeet@prl.res.in

producing enough background radiation was questioned in Refs. (Sharma (2018); Mirocha & Furlanetto (2019)).

In this work, we explore a novel possibility of cooling the gas by invoking the so-called alpha-effect. In a conventional plasma, the alpha-effect occurs due to the twisting of magnetic field lines by eddies generated due to the turbulence (Sur et al. (2008); Brandenburg & Subramanian (2007)). Here we note that magnetohydrodynamics (MHD) has been studied in the earlier literature from the time of recombination (around redshift $z \sim 1100$) to a very late period of time. In these work, the authors have studied decay of the primordial magnetic field by turbulent decay and the ambipolar diffusion (Sethi & Subramanian (2005); Chluba et al. (2015); Minoda et al. (2019)). In turbulence, the twisting of magnetic field lines by eddies in absence of mirror symmetry can enhance the magnetic field. This would give rise to the alpha-effect (Sur et al. (2008); Brandenburg & Subramanian (2007)) and the magnetic field enhances at the cost of gas energy. In the present work, we demonstrate that inclusion of this new effect can change slope of gas temperature and thereby it may help in explaining the EDGES signal. In the early Universe such an effect arises due to parity-violating process over a very wide energy scales (Joyce & Shaposhnikov (1997); Giovannini & Shaposhnikov (1998); Bhatt & Pandey (2016); Yamamoto (2016); Boyarsky et al. (2012)). This can give rise to helical primordial magnetic fields. Here, we note that alpha-effect may not require any new physics in terms of dark matter. However, the presence of a helical magnetic field is required. Indeed, the primordial magnetic fields (PMFs) generated in the early Universe due to some high energy process may have helical behaviour and violation of parity (Joyce & Shaposhnikov (1997); Giovannini & Shaposhnikov (1998); Bhatt & Pandey (2016)). These fields can survive in later times (Boyarsky et al. (2012); Bhatt & Pandey (2016)). We believe that this effect can contribute positively to explain the EDGES observations. Additionally, this 21-cm absorption signal can be used as a probe for PMFs strength at the present time in the Universe. In the previous studies, upper bound on the strength of the magnetic fields is constrained for the various cosmological scenarios (for a detailed review see Refs. Kronberg (1994); Neronov & Vovk (2010); Trivedi et al. (2012); Sethi & Subramanian (2005); Cheng et al. (1996); Grasso & Rubinstein (2001); Neronov & Vovk (2010); Ade et al. (2016); Tashiro & Sugiyama (2006); Matese & O'Connell (1969); Greenstein (1969)). In the context of EDGES signal, constraints on the magnetic fields (MFs) with upper bound of $\lesssim 10^{-10}$ G has been studied by authors of the Ref. (Minoda et al. (2019)). By invoking baryon dark-matter interaction this upper bound modifies to $\lesssim 10^{-6}$ G (Bhatt et al. (2020)). Also, the lower bound on the magnetic field strength found in Refs. (Ellis et al. (2019); The FLAT Collaboration & Biseau (2018); Tavecchio et al. (2010)). In the present work, we argue that the presence of helical magnetic fields and a lack of mirror symmetry implied by the earlier work (Joyce & Shaposhnikov (1997); Giovannini & Shaposhnikov (1998); Bhatt & Pandey (2016); Yamamoto (2016); Boyarsky et al. (2012)) can give rise to the alpha-effect around redshift $z \sim 1000$ together with the turbulent decay considered in Refs. (Minoda et al. (2019); Sethi & Subramanian (2005)).

To compute the 21-cm differential brightness temperature, T_{21} , we use **21cmFAST** code. We modify this code by adding 'decay' rates related with turbulence and ambipolar effects associated with the magnetic field together with the alpha effect. Following definition of T_{21} given in Refs. (Furlanetto & Pritchard (2006); Mesinger

& Furlanetto (2007); Mesinger et al. (2011)), we write,

$$T_{21} = 27x_{\text{HI}} \frac{1}{1 + \partial_r v_r / H} (1 + \delta_{\text{nl}}) \left(\frac{\Omega_{\text{M}} h^2}{0.15} \right)^{-1/2} \left(\frac{\Omega_{\text{b}} h^2}{0.023} \right) \times \left(\frac{1+z}{10} \right)^{1/2} \left(1 - \frac{T_{\text{CMB}}}{T_s} \right) \text{mK}, \quad (1)$$

where, x_{HI} is the neutral hydrogen fraction, $\partial_r v_r$ is the comoving derivative of LOS component of the comoving velocity, $H \equiv H(z)$ is the Hubble expansion rate and $\delta_{\text{nl}} \equiv \delta_{\text{nl}}(\mathbf{x}, z)$ is the density contrast. We take the following values for the cosmological parameters: $\Omega_{\text{M}} = 0.31$, $\Omega_{\text{b}} = 0.048$, $h = 0.68$, $\sigma_8 = 0.82$, $n_s = 0.97$ and $T_{\text{CMB}|z=0} = T_0 = 2.726$ K (Planck Collaboration (2018); Fixsen (2009)). The spin temperature T_s is defined via hydrogen number densities in 1S triplet (n_1) and singlet (n_0) hyperfine levels: $n_1/n_0 = g_1/g_0 \times \exp(-2\pi\nu_{10}/T_s)$, here, g_1 and g_0 are spin degeneracy in triplet and singlet states respectively and ν_{10} is corresponding frequency for hyperfine transition. We write T_s (Furlanetto & Pritchard (2006); Pritchard & Loeb (2012)),

$$T_s^{-1} = \frac{T_{\text{CMB}}^{-1} + x_{\alpha} T_{\alpha}^{-1} + x_c T_{\text{gas}}^{-1}}{1 + x_{\alpha} + x_c}. \quad (2)$$

Here, $T_{\alpha} \approx T_{\text{gas}}$ is the colour temperature (Wouthuysen (1952); Field (1958)). x_{α} and x_c are Wouthuysen-Field (WF) and collisional coupling coefficients respectively (Wouthuysen (1952); Field (1958); Hirata (2006); Mesinger et al. (2011)). We consider that first stars were formed at redshift $z \sim 30$. Later, their Ly α background can cause the hyperfine transition and X-ray produced by these sources start to heat the gas (Furlanetto & Pritchard (2006); Ghara & Mellema (2019); Mirocha & Furlanetto (2019); Mesinger et al. (2011, 2013); Fialkov et al. (2016); Park et al. (2019)). For this work, we take the fiducial model as defined in the Ref. (Mesinger et al. (2011)). Following the above References, we switch on the effect of Lyman α background and structure formation on T_{gas} after $z = 30$. It is important to note here that in Ref. (Venumadhav et al. (2018)), the authors have claimed that T_{gas} values can be even higher, without X-ray heating, if one incorporates indirect energy transfer from radio photons to the random motions of the gas.

In the presence of magnetic fields thermal evolution of the gas can modify. We follow the Refs. (Shu (1992); Sethi et al. (2008); Schleicher et al. (2008); Sethi & Subramanian (2005); Chluba et al. (2015)), and write the temperature evolution of the gas in presence of PMFs as,

$$\frac{dT_{\text{gas}}}{dz} = 2 \frac{T_{\text{gas}}}{1+z} + \frac{\Gamma_c}{(1+z)H} (T_{\text{gas}} - T_{\text{CMB}}) - \frac{2(\Gamma_{\text{turb}} + \Gamma_{\text{ambi}} + \Gamma_{\text{alph}})}{3N_{\text{tot}}(1+z)H}, \quad (3)$$

where, N_{tot} is the total number density of the gas i.e. $N_{\text{H}}(1 + f_{\text{He}} + X_c)$, N_{H} is the neutral hydrogen number density, $f_{\text{He}} \propto \infty$

(2005); Chluba et al. (2015)),

$$\Gamma_{\text{ambi}} \approx \frac{(1 - X_e)}{\gamma X_e (M_H N_b)^2} \frac{E_B^2 f_L (n_B + 3)}{L_d^2}, \quad (4)$$

$$\Gamma_{\text{turb}} = \frac{1.5 m [\ln(1 + t_i/t_d)]^m}{[\ln(1 + t_i/t_d) + 1.5 \ln\{(1 + z_i)/(1 + z)\}]^{m+1}} H E_B, \quad (5)$$

here, the coupling coefficient $\gamma = 1.9 \times 10^{14} (T_{\text{gas}}/\text{K})^{0.375} \text{cm}^3/\text{g/s}$, M_H is mass of Hydrogen atom, N_b is baryon number density, $f_L(x) = 0.8313(1 - 1.020 \times 10^{-2}x)x^{1.105}$, $t_i/t_d \approx 14.8(1 + z)(nG/B_0)(L_d/\text{Mpc})$, $m = 2(n_B + 3)/(n_B + 5)$, $z_i = 1088$ is the initial redshift when heating starts & L_d is the coherence length scale of the magnetic field. It is constrained by Alfvén wave damping length scale, $L_d = 1/[k_d(1 + z)]$. Magnetic fields at length-scales smaller than L_d are strongly damped by the radiative-viscosity (Sethi & Subramanian (2005); Jedamzik et al. (1998); Chluba et al. (2015); Kunze & Komatsu (2014)),

$$k_d \approx 286.91 \left(\frac{nG}{B_0} \right) \text{Mpc}^{-1} \quad (6)$$

where, B_0 is the present day magnetic field strength.

The process of inverse cascade in presence of the α -effect has been studied in cosmology literature where magnetic energy flows from smaller length scales to the larger length scale (Christensson et al. (2001); Pavlović et al. (2017); Olesen (1997)). It is found that the typical comoving length scales at which the coherent primordial magnetic field can exist is around few Mpc. Strength of PMFs is constrained by Planck collaboration on the length scale of 1 Mpc (Planck Collaboration et al. (2014)). We consider power-spectrum of the PMFs as a power law $P_B(k) = Ak^{n_B}$ for $k < k_d$ and $P_B(k) = 0$ for $k \geq k_d$. Amplitude of the PMFs smoothed over length scale λ , $B_\lambda^2 = \int_0^\infty (dk/2\pi)^3 P_{B,0}(k) \exp(-k^2 \lambda^2) = (\sqrt{2}/(k_d \lambda))^{n_B+3} B_0^2$ (Caprini et al. (2004); Chluba et al. (2015); Planck Collaboration et al. (2014)). For a nearly scale invariant magnetic spectral index, $n_B = -2.9$ and $\lambda = 1$ Mpc, using the above relation for B_λ^2 , one can estimate the amplitude of PMFs at 1 Mpc ($B_{1\text{Mpc}}$) (Chluba et al. (2015)). The magnetic field energy density, $E_B = B^2/(8\pi)$, in presence of the alpha-effect,

$$\frac{dE_B}{dz} = 4 \frac{E_B}{1+z} + \frac{1}{(1+z)H} \left[\Gamma_{\text{turb}} + \Gamma_{\text{ambi}} - \frac{\alpha}{4\pi} |\mathbf{B} \cdot (\nabla \times \mathbf{B})| \right]. \quad (7)$$

Here, $\mathbf{B} \equiv \langle \mathbf{B} \rangle$. Following Refs. (Sur et al. (2008); Brandenburg & Subramanian (2007, 2005)), if the magnetic Reynolds number is large enough, $\alpha = (1/3)u_{\text{rms}}$. Here we use Equipartition theorem– $u_{\text{rms}}^2 = 3T_{\text{gas}}/M_H$. Following Ref. (Schleicher et al. (2008); Caprini et al. (2004)), we approximate last term in equation (7) as

$$|\mathbf{B} \cdot (\nabla \times \mathbf{B})| \approx \frac{B^2}{L_d}. \quad (8)$$

Thus, in equation (7),

$$\Gamma_{\text{alph}} \approx -2 \left(\frac{T_{\text{gas}}}{3M_H} \right)^{1/2} \frac{E_B}{L_d}. \quad (9)$$

Here we note that in addition to the usual expansion term in Eq. (7), the terms with coefficients Γ_{turb} and Γ_{ambi} also contribute towards the decay of magnetic fields. But, the term with factor α has sign opposite to the decay terms and this will help the magnetic field to survive for a longer duration. However, the decay terms will eventually dominate over the α -effect.

2 RESULT AND DISCUSSION

Ignoring logarithmic dependency of turbulent decay, it evolves as $\Gamma_{\text{turb}} \propto (1+z)^{5.2}$, ambipolar diffusion $\Gamma_{\text{ambi}} \propto (1+z)^{3.63}(1-X_e)/X_e$ at early time since $T_{\text{gas}} \propto (1+z)$ and after $z \lesssim 100$ it evolves as $\propto (1+z)^{3.25}/X_e$ because of $T_{\text{gas}} \propto (1+z)^2$ and $X_e \ll 1$ at late time. Magnetic energy rate due to the alpha-effect, Γ_{alph} , is $\propto (1+z)^{5.5}$ for $z \gtrsim 100$ otherwise it's $\propto (1+z)^6$. Therefore, we expect cooling due to the alpha-effect is more effective than heating due to the turbulent decay. After that, at late time ($z < 100$) the ambipolar diffusion is more effective (also depends on PMFs strength). Thus, the gas temperature will fall quickly in comparison with the standard scenario–heating/cooling due to magnetic fields is not included. As shown in Refs. (Minoda et al. (2019); Chluba et al. (2015)) in presence of a helical magnetic field Γ_{turb} dominates over Γ_{ambi} for $z > 100$. Presence of the alpha effect can also be felt very strongly for this range of the redshift. One can write $\frac{\Gamma_{\text{alph}}}{\Gamma_{\text{ambi}}} \sim 1.48 \left(\frac{T_{\text{gas}}}{\text{Kelvin}} \right)^{0.875} \frac{X_e}{1-X_e} (1+z) \left(\frac{nG}{B_0} \right)$. The growth in the magnetic energy density due to α -effect in the present scenario can be estimated as follows: From equation (3) and (7),

$$\frac{dT_{\text{gas}}}{dz} = \frac{dT_{\text{gas}}}{dz} \Big|_{\text{std}} - \frac{2}{3N_{\text{tot}}} \left[\frac{dE_B}{dz} - \frac{dE_B}{dz} \Big|_{\text{std}} \right], \quad (10)$$

where, $\frac{dT_{\text{gas}}}{dz} \Big|_{\text{std}}$ represent the gas temperature evolution with redshift in absence of the magnetic fields. While, $\frac{dE_B}{dz} \Big|_{\text{std}} = 4 \frac{E_B}{1+z}$, represent the magnetic field energy density evolution with redshift without any α -effect, turbulent decay and ambipolar diffusion. For example, in figure (1), maximum transformation of thermal energy to magnetic energy happens at $z \approx 58$ for $B_0 = 6 \times 10^{-3}$ nG. Now using equation (10) and results of plot (1) one can find E_B and which gives $B \Big|_{z=58} \approx 4 \times 10^{-7}$ G. The upper constraint from Planck results on the present day value of magnetic field is around 4.1×10^{-9} G, from which one can estimate magnetic field at $z = 58$ around 1.4×10^{-5} G. Thus, the magnetic field generated by the α -effect is consistent with Planck bound (Planck Collaboration et al. (2014)).

To study the magnetic heating (cooling) of the gas we use the code `recfast++` (Chluba et al. (2015)). In figure (1a), plots of gas temperatures for different values of B_0 are shown as function of z . The dot-dashed line represent the standard recombination history. The figure shows that as values of B_0 approaches 10^{-5} nG, T_{gas} recovers the standard thermal evolution. By increasing magnetic field from 10^{-5} nG, T_{gas} decreases. For $B_0 \approx 10^{-3}$ nG, one gets $T_{\text{gas}} < 3.2$ Kelvin for $z = 17$. Further we note that by increasing B_0 the minimum of gas temperature shifts towards higher values of the redshift. Figure (1b) shows that by increasing of B_0 from 5×10^{-3} nG, T_{gas} rises. However, gas temperature around $z = 17$ exceeds 3.2 Kelvin for $B_0 > 6 \times 10^{-3}$ nG. Therefore, desired value of magnetic field should be in the range of 5×10^{-4} nG $\lesssim B_0 \lesssim 6 \times 10^{-3}$ nG. These upper and lower bounds on B_0 are also consistent with constraints found in Refs. (Kronberg (1994); Neronov & Vovk (2010); Trivedi et al. (2012); Sethi & Subramanian (2005); Cheng et al. (1996); Grasso & Rubinstein (2001); Neronov & Vovk (2010); Ade et al. (2016); Tashiro & Sugiyama (2006); Matese & O'Connell (1969); Greenstein (1969); Minoda et al. (2019); Bhatt et al. (2020); Ellis et al. (2019); The FLAT Collaboration & Biteau (2018); Tavecchio et al. (2010)).

Further, in figure (2), we have included the X-ray heating due to first stars after the redshift $z = 30$ together with the adiabatic heating/cooling as a result of structure formation. The blue dot-dashed line indicates the T_{gas} evolution for the standard cosmological scenario and double-dot dashed line shows T_{CMB} evolution. The

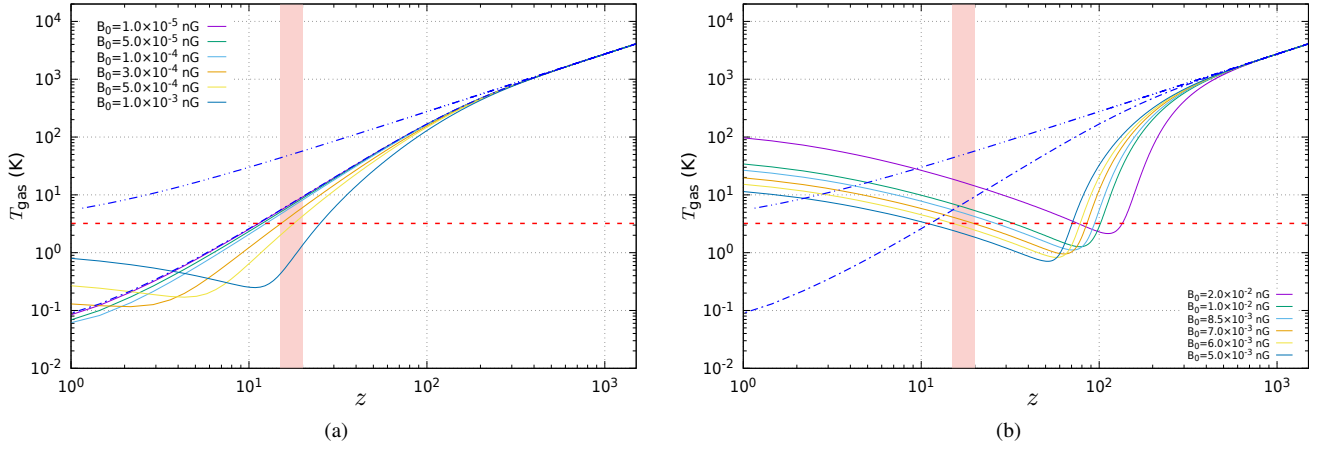


Figure 1. The gas temperature evolution with redshift for different magnetic field strengths – solid lines. The blue dot-dashed line indicates the T_{gas} evolution for the standard cosmological scenario and double-dot dashed line shows T_{CMB} evolution. The shaded region is corresponds to 21-cm absorption signal, $15 \leq z \leq 20$, reported by EDGES observation. The red dashed horizontal line is corresponds to the $T_{\text{gas}} = 3.2$ K.

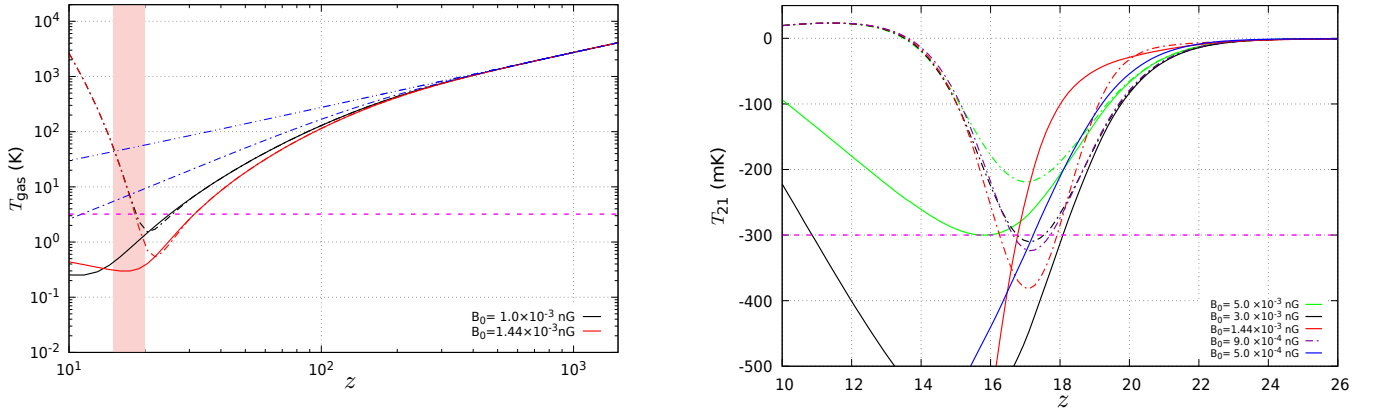


Figure 2. Black (red) solid line represent T_{gas} evolution with z in presence of magnetic field. Dot-dashed lines indicate the X-ray heating for different magnetic field strengths. The blue coloured lines represent the standard cosmological scenario. The magenta dashed line is corresponds to the $T_{\text{gas}} = 3.2$ K.

black and red solid line plots represent the case when only magnetic heating/cooling terms are included. The black and red dot-dashed line shows the cases when all these effects are present. In this case, the gas temperature rises quickly in comparison with the only magnetic heating/cooling cases. Therefore, in the presence of X-ray heating, our previously mentioned upper and lower bounds on magnetic field strength can modify.

In figure (3), we plot T_{21} as a function of redshift for different magnetic field strengths. We have considered two particular cases involving (dot-dashed lines) and without (solid lines) X-ray heating. For the X-ray heating we consider the fiducial model (Mesinger et al. (2011)). In all cases, we incorporate adiabatic heating/cooling from structure formations (Mesinger et al. (2011)). Spin temperature coupling has two main contribution, one from X-ray excitation of neutral hydrogen and other from photons emitted between Lyman to Ly α limit from the first stars. For dot-dashed line we include both coupling and for solid lines, we take only second coupling. The figure shows that without including X-ray heating, one can obtain $-1000 \text{ mK} \leq T_{21} \leq -300 \text{ mK}$. For the dot-dashed

Figure 3. 21-cm global signal in presence (dot-dashed) and absence (solid lines) of X-ray heating of gas for different magnetic field strengths. The magenta dashed line is corresponds to the EDGES upper bound on T_{21} : -300 mK .

lines, the minimum of T_{21} profile first decreases while increasing B_0 values from $\sim 9 \times 10^{-4} \text{ nG}$ and after a certain value of B_0 , minimum of T_{21} starts increasing: For $B_0 = 3 \times 10^{-3} \text{ nG}$ and $9 \times 10^{-4} \text{ nG}$ we get $T_{21} = -310 \text{ mK}$ and -323 mK at $z = 17$ respectively. This gives allowed range for B_0 to be in the range (using EDGES upper bound on T_{21}) $9 \times 10^{-4} \text{ nG} \leq B_0 \leq 3 \times 10^{-3} \text{ nG}$ after inclusion of X-ray heating.

3 CONCLUSIONS

In conclusion, we have studied 21-cm differential brightness temperature in the presence of helical primordial magnetic fields. We have shown that the presence of the alpha effect can reduce gas temperature to 3.2 Kelvin, at the center of “U” shaped profile, when present-day strength of the magnetic field is in the range $5 \times 10^{-4} \text{ nG} \leq B_0 \leq 6 \times 10^{-3} \text{ nG}$ without X-ray heating. For the case when X-ray heating is included we get $9 \times 10^{-4} \text{ nG} \leq B_0 \leq 3 \times 10^{-3} \text{ nG}$ for $T_{21} \leq -300 \text{ mK}$. Here we note that our analysis does not require any new physics in terms of dark matter.

ACKNOWLEDGEMENTS

We would like to thank the anonymous referee whose comments has helped us in improving presentation of our results. All the computations were performed on the Vikram-100 HPC cluster at PRL, Ahmedabad.

REFERENCES

- Ade P. A. R., et al., 2016, *A&A*, 594, A19
 Aristizabal Sierra D., Fong C. S., 2018, *PLB*, 784, 130
 Barkana R., 2018, *Nature*, 555, 71
 Barkana R., Outmezguine N. J., Redigolo D., Volansky T., 2018, *PRD*, 98, 103005
 Berlin A., Hooper D., Krnjaic G., McDermott S. D., 2018, *PRL*, 121, 011102
 Bhatt J. R., Pandey A. K., 2016, *PRD*, 94, 043536
 Bhatt J. R., Natwariya P. K., Nayak A. C., Pandey A. K., 2020, *Eur. Phys. J. C*, 80, 334
 Bowman J. D., Rogers A. E. E., Monsalve R. A., Mozdzen T. J., Mahesh N., 2018, *Nature*, 555, 67
 Boyarsky A., Fröhlich J., Ruchayskiy O., 2012, *PRL*, 108, 031301
 Brandenburg A., Subramanian K., 2005, *A&A*, 439, 835
 Brandenburg A., Subramanian K., 2007, *Ast. Nac.*, 328, 507
 Bransden B. H., Dalgarno A., John T. L., Seaton M. J., 1958, *Proc. Phys. Soc.*, 71, 877
 Caprini C., Durrer R., Kahnashvili T., 2004, *Phys. Rev. D*, 69, 063006
 Cheng B., Olinto A. V., Schramm D. N., Truran J. W., 1996, *PRD*, 54, 4714
 Chluba J., Thomas R. M., 2011, *MNRAS*, 412, 748
 Chluba J., Vasil G. M., Dursi L. J., 2010, *MNRAS*, 407, 599
 Chluba J., Paoletti D., Finelli F., Rubiño-Martín J. A., 2015, *MNRAS*, 451, 2244
 Christensson M., Hindmarsh M., Brandenburg A., 2001, *Phys. Rev. E*, 64, 056405
 Ellis J., Fairbairn M., Lewicki M., Vaskonen V., Wickens A., 2019, *JCAP*, 2019, 019
 Ewall-Wice A., Chang T.-C., Lazio J., Doré O., Seiffert M., Monsalve R. A., 2018, *ApJ*, 868, 63
 Fialkov A., Cohen A., Barkana R., Silk J., 2016, *MNRAS*, 464, 3498
 Field G. B., 1958, *Proceedings of the IRE*, 46, 240
 Fixsen D. J., 2009, *ApJ*, 707, 916
 Fraser S., et al., 2018, *PLB*, 785, 159
 Furlanetto S. R., Pritchard J. R., 2006, *MNRAS*, 372, 1093
 Ghara R., Mellema G., 2019, *MNRAS*, 492, 634
 Giovannini M., Shaposhnikov M. E., 1998, *PRD*, 57, 2186
 Grasso D., Rubinstein H. R., 2001, *Phys. Rept.*, 348, 163
 Greenstein G., 1969, *Nature*, 223, 938
 Hart L., Chluba J., 2018, *MNRAS*, 474, 1850
 Hirata C. M., 2006, *MNRAS*, 367, 259
 Jedamzik K., Katalinić V. c. v., Olinto A. V., 1998, *Phys. Rev. D*, 57, 3264
 Joyce M., Shaposhnikov M., 1997, *PRL*, 79, 1193
 Kovetz E. D., Poulin V., Gluscevic V., Boddy K. K., Barkana R., Kamionkowski M., 2018, *PRD*, 98, 103529
 Kronberg P., 1994, *Rep. Prog. Phys.*, 57, 325
 Kunze K. E., Komatsu E., 2014, *JCAP*, 2014, 009
 Matese J. J., O'Connell R. F., 1969, *Phys. Rev.*, 180, 1289
 Mesinger A., Furlanetto S., 2007, *ApJ*, 669, 663
 Mesinger A., Furlanetto S., Cen R., 2011, *MNRAS*, 411, 955
 Mesinger A., Ferrara A., Spiegel D. S., 2013, *MNRAS*, 431, 621
 Minoda T., Tashiro H., Takahashi T., 2019, *MNRAS*, 488, 2001
 Mirocha J., Furlanetto S. R., 2019, *MNRAS*, 483, 1980
 Moroi T., Nakayama K., Tang Y., 2018, *PLB*, 783, 301
 Muñoz J. B., Loeb A., 2018, *Nature*, 557, 684
 Muñoz J. B., Dvorkin C., Loeb A., 2018, *PRL*, 121, 121301
 Neronov A., Vovk I., 2010, *Science*, 328, 73
 Olesen P., 1997, *Physics Letters B*, 398, 321
 Park J., Mesinger A., Greig B., Gillet N., 2019, *MNRAS*, 484, 933
 Pavlović P., Leite N., Sigl G., 2017, *Phys. Rev. D*, 96, 023504
 Planck Collaboration 2018, [arXiv:1807.06209](https://arxiv.org/abs/1807.06209)
 Planck Collaboration et al., 2014, *A&A*, 571, A16
 Pritchard J. R., Loeb A., 2012, *Rep. Prog. Phys.*, 75, 086901
 Schleicher D. R. G., Banerjee R., Klessen R. S., 2008, *Phys. Rev. D*, 78, 083005
 Seager S., Sasselov D. D., Scott D., 1999, *Ast. J.*, 523, L1
 Seager S., Sasselov D. D., Scott D., 2000, *ApJ*, 128, 407
 Sethi S. K., Subramanian K., 2005, *MNRAS*, 356, 778
 Sethi S. K., Nath B. B., Subramanian K., 2008, *MNRAS*, 387, 1589
 Sharma P., 2018, *MNRAS Lett.*, 481, L6
 Shu F. H., 1992, The physics of astrophysics. Volume II: Gas dynamics.. ISBN 0-935702-65-2, <http://adsabs.harvard.edu/abs/1992pavi.book.....S>
 Sikivie P., 2019, *Physics of the Dark Universe*, 24, 100289
 Slatyer T. R., Wu C.-L., 2018, *PRD*, 98, 023013
 Sur S., Brandenburg A., Subramanian K., 2008, *MNRAS Lett.*, 385, L15
 Tashiro H., Sugiyama N., 2006, *MNRAS*, 368, 965
 Tashiro H., Kadota K., Silk J., 2014, *PRD*, 90, 083522
 Tavecchio F., Ghisellini G., Foschini L., Bonoli G., Ghirlanda G., Coppi P., 2010, *MNRAS: Letters*, 406, L70
 The FLAT Collaboration Biteau J., 2018, *ApJS*, 237, 32
 Trivedi P., Seshadri T. R., Subramanian K., 2012, *PRL*, 108, 231301
 Venumadhav T., Dai L., Kurov A., Zaldarriaga M., 2018, *PRD*, 98, 103513
 Wouthuysen S. A., 1952, *apj*, 57, 31
 Yamamoto N., 2016, *Phys. Rev. D*, 93, 065017

This paper has been typeset from a $\text{\TeX}/\text{\LaTeX}$ file prepared by the author.